IL NUOVO CIMENTO **39 C** (2016) 397
DOI 10.1393/ncc/i2016-16397-3

Colloquia: IWM-EC 2016

Impact of pairing on clustering and neutrino transport properties in low-density stellar matter

S. Burrello([1])([2]), M. Colonna([1]) and F. Matera([3])

([1]) *INFN, Laboratori Nazionali del Sud - Catania, Italy*
([2]) *Dipartimento di Fisica e Astronomia, Università di Catania - Catania, Italy*
([3]) *Dipartimento di Fisica e Astronomia, Università di Firenze and INFN - Firenze, Italy*

received 10 January 2017

Summary. — We analyze the effects of pairing correlations on the behavior of stellar matter, focusing on thermodynamical conditions close to the onset of the liquid–gas phase transition, which are characterized by quite large density fluctuations and where clustering phenomena occur. We concentrate on the neutrino transport properties and we show, within a thermodynamical treatment, that at moderate temperatures, where pairing effects are still active, the scattering of neutrinos in the nuclear medium is significantly affected by the matter superfluidity. The pairing correlations can indeed enhance neutrino trapping and reduce the energy flux carried out by neutrino emission. New hints about an important impact of pairing on the cooling mechanism, by neutrino emission, are so envisaged and therefore this study could be of relevant interest for the evolution of proto-neutron stars and in modelization of supernova explosions.

Neutrino interaction in a low-density and neutron-rich nuclear medium plays a crucial role in core-collapse supernovae [1] and in the early thermal relaxation phase of newly formed neutron star crust [2]. The neutrino emission is in fact the only direct probe of the mechanism of supernovae and the structure of proto-neutron stars [3, 4].

Many efforts have therefore been recently devoted to accurately describe the neutrino production and interaction and it has been shown that these processes are significantly influenced by some characteristic features of interacting many-body systems, such as phase transitions [5-8]. For nuclear matter at sub-saturation density and relatively low temperature ($T \lesssim 15\,\mathrm{MeV}$), in particular, a liquid-gas phase transition is expected to emerge, according to the mechanical (spinodal) instability exhibited by the nuclear mean field [9]. Such a phenomenon is strictly connected to the multifragmentation process observed in heavy-ion collisions at Fermi energies [10] and to the emergence of clustering phenomena in compact stars [11]. Moreover, it came quite recently out that large density fluctuations developing at the spinodal border strongly increase the neutrino scattering [12]. As a result, neutrinos could be trapped in a thin layer of the star, so that their emissivity in the low-density region should be deeply quenched.

As another general feature, fermionic systems may also exhibit pairing correlations, which are a key ingredient to describe the cooling process and glitch phenomena of compact stellar objects [13]. Since these correlations are active at low density and moderate temperature, there exists a region of the nuclear matter phase diagram where volume instabilities overlap with quite important superfluid effects [14].

The aim of this work is hence to investigate how the pairing correlations can affect the neutrino scattering in nuclear medium, in conditions close to the onset of the liquid-vapor phase transition, which are encountered in proto-neutron stars, as well as in the pre-bounce phase of supernova explosions, whereas the temperature is still rather low.

Owing to its global isoscalar-like character [15], the spinodal instability leads to an enhancement of the density response function, which modifies the neutral current neutrino scattering, leaving the charged current absorption unaltered [17].

Thus, in the following, we consider nonrelativistic nucleons coupled to neutrinos through only the neutral current and we limit in particular only to its vector part, since the axial neutral current is not affected.

Then the differential cross section (per unit of volume V) for scattering in the medium of neutrinos with energy E_ν, as a function of the neutrino final energy E'_ν and scattering angle θ, is given by [16]

$$\frac{1}{V}\frac{\mathrm{d}^3\sigma}{\mathrm{d}E'_\nu \mathrm{d}\Omega^2} = \frac{G_F^2}{8\pi^3}\left(E'_\nu\right)^2 (1+\cos\theta)\, S_V^{00}(\omega,\mathbf{q}). \tag{1}$$

In the latter equation, $\omega = E_\nu - E'_\nu$ denotes the energy transfer to the medium, $\mathbf{q}$ is the momentum transfer, which is related to ω and to the neutrino scattering angle θ (we use units such that $\hbar = c = k_B = 1$), G_F denotes the weak coupling constant and S_V^{00} identifies the dynamic form factor, which can be expressed in terms of the nucleon density-density correlation factor as

$$S_V^{00}(\omega,\mathbf{q}) = \int \mathrm{d}t\, \mathrm{d}\mathbf{r}\, e^{i\omega t}\, e^{-i\mathbf{q}\cdot\mathbf{r}} \langle J^{(N)0}(t,\mathbf{r}) J^{(N)0}(0,0)\rangle, \tag{2}$$

where $J_0^{(N)}(t,\mathbf{r}) = \sum_{i=n,p} c_V^{(i)} \rho_i(t,\mathbf{r})$, with $c_V^{(n)} = -0.5$, $c_V^{(p)} = 0.036$ and $\rho_i(t,\mathbf{r})$ $(i = n,p)$ the nucleon (neutron or proton) local density.

Since in the heavy nucleons limit all the factors except $S_V^{00}(\omega,\mathbf{q})$ can be evaluated at $\omega = 0$ [17], the integration of (1) on a range of ω values leads to

$$\delta(\omega) \int \mathrm{d}\omega' S_V^{00}(\omega',\mathbf{q}) = 2\pi\delta(\omega) S_V^{00}(\mathbf{q}), \tag{3}$$

where $S_V^{00}(\mathbf{q})$ is the static structure factor, which corresponds to nucleon-nucleon density fluctuation correlations taken at equal time:

$$S_V^{00}(\mathbf{q}) = \langle \delta J^{(N)\,0}(\mathbf{q}) \delta J^{(N)\,0}(-\mathbf{q})\rangle. \tag{4}$$

Such a quantity, by exploiting the fluctuation-dissipation theorem [18] and neglecting quantal fluctuations, is given by

$$S_V^{00}(\mathbf{q}) = T\left[{c_V^{(n)}}^2 \mathbf{C}_{nn}^{-1}(q) + {c_V^{(p)}}^2 \mathbf{C}_{pp}^{-1}(q) + 2 c_V^{(n)} c_V^{(p)} \mathbf{C}_{np}^{-1}(q)\right], \tag{5}$$

where T is the temperature of the system and $\mathbf{C}^{-1}$ is the inverse of the curvature matrix of the system free energy density [17].

In this paper, we consider a stellar matter with a globally neutral charge whose local energy density, which is a function of the total density $\rho = \rho_n + \rho_p$, the proton fraction $y_p = \rho_p/\rho$ and the electron density ρ_e, can be written as

$$\mathcal{E}_{tot}(\rho, y_p, \rho_e) = \mathcal{E}_{NM} + \mathcal{E}^f_{NM} + \mathcal{E}_{Coul} + \mathcal{E}_e(\rho_e), \tag{6}$$

where $\mathcal{E}_e$ is the energy density associated with the electron kinetic energy and the contributions of the Coulomb term, $\mathcal{E}_{Coul}$, related to the interaction between all charges (protons and electrons), and of surface terms, $\mathcal{E}^f_{NM}$, are explicitly evidenced.

The electron term is evaluated in the approximation of a degenerate and ultrarelativistic Fermi gas, while the spin-saturated nuclear matter energy density, $\mathcal{E}_{NM}$, in the BCS approximation reads [14, 19]

$$\mathcal{E}_{NM}(\rho, y_p) = \sum_{i=n,p} \left[2 \int \frac{\mathrm{d}\mathbf{p}}{(2\pi)^3} f_i \frac{p^2}{2m_i^*} + \frac{1}{4} v_\pi(\rho_i) |\tilde{\rho}_i|^2 \right] + \mathcal{E}_{Sky}. \tag{7}$$

In the previous equation, f_i is the occupation number for a nucleon of species i with momentum $\mathbf{p}$ and $\tilde{\rho}_i = 2\Delta_i/v_\pi$ denotes the anomalous density associated with the pairing gap Δ_i. The quasiparticle energies in the definition of f_i are given by $E_{\Delta,i} = \sqrt{\xi_i^2 + \Delta_i^2}$, where $\xi_i = p^2/2m_i^* - \mu_i + U_i$, being μ_i and $U_i = (\frac{\partial \mathcal{E}_{NM}}{\partial \rho_i})_{\tilde{\rho}_i}$ the chemical and mean-field potential, respectively, of each nucleonic species i.

We employ the SAMi-J35 Skyrme parametrization [20] for the local energy density $\mathcal{E}_{Sky}$ and the effective nucleon mass m_i^*. For the pairing term, we adopt the same functional form as in [19, 14], whose density-dependent strength, $v_\pi(\rho_i)$, is calculated by inverting the gap equation, in order to reproduce the ${}^1S_0$ pairing gap, as obtained by Brueckner-Hartree-Fock calculations in pure neutron matter [21]. We assume moreover that the pairing interaction acts only between nucleons of the same type, because np pairing is strongly suppressed in asymmetric matter. The results are then extended to the pp case, assuming that the pairing strength is the same as in the nn case, just depending on the density of the species considered.

Within this framework, one can easily evaluate the components of the curvature matrix $\mathbf{C}$

$$\mathbf{C}(q) = \begin{pmatrix} \partial_{\rho_n}\mu_n & \partial_{\rho_p}\mu_n & 0 \\ \partial_{\rho_n}\mu_p & \partial_{\rho_p}\mu_p & 0 \\ 0 & 0 & \partial_{\rho_e}\mu_e \end{pmatrix} + 2q^2 \begin{pmatrix} C^f_{nn} & C^f_{np} & 0 \\ C^f_{pn} & C^f_{pp} & 0 \\ 0 & 0 & 0 \end{pmatrix} + \frac{4\pi e^2}{q^2} \begin{pmatrix} 0 & 0 & 0 \\ 0 & 1 & -1 \\ 0 & -1 & 1 \end{pmatrix}, \tag{8}$$

where $e^2 = 1.44\,\mathrm{MeV}\cdot\mathrm{fm}$ and C^f_{ij} are combinations of Skyrme surface parameters [22].

The pairing interaction modifies the neutron and proton chemical potential derivatives [14] and so, in suitable thermodynamical conditions, it can affect the neutrino differential cross section (1).

As mentioned before, neutrino trapping is associated with the large density fluctuations emerging close to the spinodal border. In the framework depicted above, the amplitude of density fluctuations is connected to the inverse of the eigenvalues of the curvature matrix and, in particular, they are larger when the isoscalar-like one, $\lambda_S(q)$, is small. In this case, pairing correlations could have a significant influence on the curvature matrix

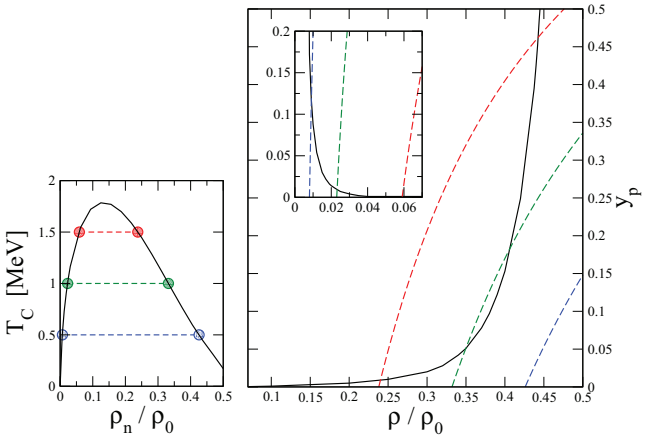

Fig. 1. – Left panel: The critical temperature for the superfluid/normal phase transition, as a function of the reduced neutron density ρ_n/ρ_0. Right panel: The spinodal border (full line), in the (ρ, y_p)-plane, associated with temperature $T = 0.5\,\mathrm{MeV}$ and momentum transfer $q = 30\,\mathrm{MeV}$. The inset shows a zoom of the low-density region. The dashed lines are curves of constant neutron density, corresponding to the values associated with the circles in the left panel (see text for more details).

elements, especially in correspondence of the critical temperature T_c of the superfluid phase transition, where discontinuities appear in chemical potential derivatives [14].

In fig. 1 (left panel) we represent the neutron critical temperature, $T_c^n \simeq 0.567\Delta_n$, as a function of the neutron density. The right panel shows the spinodal border (full line), in the (ρ, y_p)-plane, at typical temperature and q values for our study. Limiting, for sake of simplicity, the explanation only to the neutron pairing case, for each fixed temperature in the plot on the left panel, one identifies two values of the neutron densities for which the temperature considered corresponds to the critical one and pairing effects are expected to be large. Each value of the neutron density defines an hyperbole in the (ρ, y_p)-plane (dashed lines on the right panel), so that the crossing with the spinodal border allows to find the density-asymmetry regions where large density fluctuations can coexist with important pairing contributions. Several thermodynamical states are identified, from very small densities up to $\rho \approx 0.4\rho_0$ (being $\rho_0 = 0.16\,\mathrm{fm}^{-3}$ the saturation density) with a wide range of proton fractions. These conditions coincide with those encountered in the inner crust of a proto-neutron star or in the pre-bounce phase of a supernova explosion, when the temperature is still quite low (see, *e.g.*, refs. [23-25]).

In order to consider two different density regimes, following the previous analysis, we present the results obtained for: 1) $\rho = \rho_0/100$, at $T = 0.5\,\mathrm{MeV}$, and 2) $\rho = \rho_0/4$, at $T = 1.4\,\mathrm{MeV}$, focusing on temperature values where large pairing effects are expected. Several y_p values are considered, around to the values suggested by fig. 1. Since the temperatures considered in the two different scenarios are both above the proton critical ones, only neutrons are paired.

Figure 2 (left panel) illustrates the neutrino differential cross section, $\sigma_{VE} \equiv 1/(VE_\nu^2)\mathrm{d}^2\sigma/\mathrm{d}\Omega^2$ (full lines), as a function of the neutrino energy E_ν and at a scattering θ angle such that $q = E_\nu$. To stress pairing effects, the results are shown together with the calculations achieved by neglecting the pairing interaction (dashed lines).

One can observe that, due to Coulomb repulsion, at small momentum transfer q values, the eigenvalue $\lambda_S(q)$ is always positive and so the density oscillations are stable.

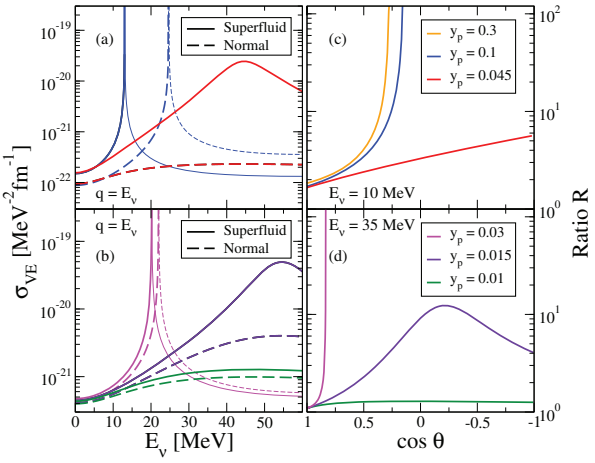

Fig. 2. – Left panels: Neutrino differential cross sections, σ_{VE} (see text), as a function of the neutrino energy E_ν, obtained in the full calculation (full lines) or neglecting the pairing interaction (dashed lines). Right panels: Ratio R between the full calculation and the results obtained neglecting the pairing interaction, as a function of the cosine of the neutrino scattering angle θ, for selected neutrino energies. Results are shown for the following conditions: $\rho = \rho_0/100$, $T = 0.5\,\mathrm{MeV}$ (panels (a) and (c)) and $\rho = \rho_0/4$, $T = 1.4\,\mathrm{MeV}$ (panels (b) and (d)). The proton fractions considered are indicated inside the figure.

Actually, at the lowest density considered (case 1), panel (a)), the proton fraction $y_p = 0.045$ corresponds to stable conditions for all q values. Within such a thermodynamical configuration, in fact, the density oscillations are not much influenced by Coulomb (acting at small q's) or surface (acting at large q's) effects, so that λ_S remains close to zero for an appreciable range of the momentum transfer and the relative weigth of pairing effects is clearly enhanced. As a consequence, an important influence of superfluidity emerges on the cross section, especially for intermediate neutrino energies, where a bump is observed. On the contrary, for the higher proton fraction case (see the result for $y_p = 0.1$), nuclear matter crosses the spinodal border already for oscillations having low momentum transfer and a divergent behavior is observed for density fluctuations and neutrino cross section. Of course, one could carefully evaluate these density fluctuations going beyond the curvature of the free energy, on the other hand one should to remark that already a this level a strong pairing effect on the neutrino opacity comes out. As a quite general result, in fact, one can observe that pairing interaction significantly reduce the curvature of the free energy density. Correspondingly, density fluctuations and neutrino cross section are appreciably increased and one can conclude that neutron correlations favours matter clustering. One can notice, moreover, that pairing correlations cause a non-negligible shift to smaller values of the neutrino energy associated with the divergency in the full calculations. This implies that also less energetic neutrinos have more chances to be trapped, so that the energy flux carried away by neutrinos is necessary damped.

For $y_p = 0.1$, larger transfer momenta q's correspond instead to unstable oscillations and, since $\lambda_S(q)$ is negative, it does not hold the prescription given in eq. (5) to evaluate neutron and proton density fluctuations. Indeed, while the variance associated with isoscalar-like stable fluctuations reads as $\sigma_S(q) = T/\lambda_S(q)$, in presence of instabilities

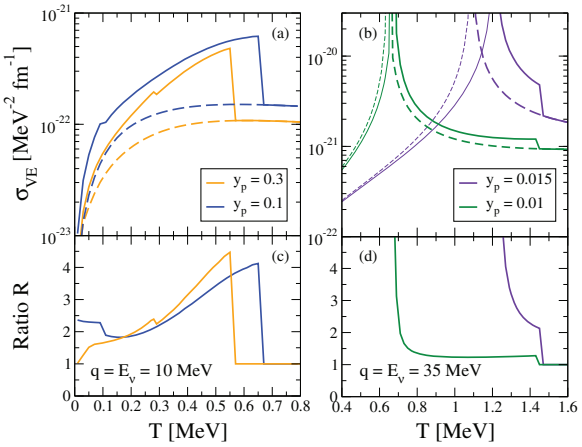

Fig. 3. – Top panels: Neutrino differential cross section, σ_{VE} (see text), as a function of the temperature T, as obtained in the full calculation (full lines) or neglecting the pairing interaction (dashed lines). Bottom panels: Ratio R between the full calculation and the results obtained neglecting the pairing interaction, as a function of the temperature T. Results are shown for the following conditions: $\rho = \rho_0/100$ (panels (a) and (c)) and $\rho = \rho_0/4$ (panels (b) and (d)). The proton fractions considered are indicated inside the figure.

it grows exponentially with time to reach a new equilibrium condition, corresponding to the clustered matter [9]. Therefore, the equilibrium fluctuations inside the spinodal region cannot be exactly estimated within our framework, but assuming, as a first-order approximation, that are close to the value obtained, for each q, at the instability growth time $\tau(q)$ [26], one gets $\sigma_S(q) \approx T/|\lambda_S|$ and so the curvature matrix components, eq. (8), are accordingly modified. The corresponding neutrino cross sections are indicated by thin lines in fig. 2.

The panel (b) illustrates the results obtained for case 2), where a smaller proton fractions y_p is taken, as indicated by the analysis shown in fig. 1. We mention that this also corresponds to the trend predicted for the proton fraction in the inner crust of neutron stars [11, 25].

In the latter case pairing effects, though still quite significant, are reduced with respect to the previous case, since they are also linked to the density derivative of the pairing gap (and thus of the critical temperature), which is steeper for case 1) [14]. In order to emphasize the role of pairing effects, panels (c), (d) of fig. 2 represent, for the stable q values, the ratio R between the cross section associated with the full calculations and the results obtained neglecting the pairing interaction, as a function of the cosine of θ, for neutrino energies compatible with β-equilibrium conditions. It clearly emerges how important is the impact of the pairing when approaching the spinodal border.

The influence of the temperature on our results is discussed in fig. 3, where the quantity σ_{VE} is displayed, in full calculation and neglecting the pairing interaction, for selected neutrino energies and $q = E_\nu$ and for density conditions as in case 1) (panel (a)) and case 2) (panel (b)). Pairing effects appear quite important already at very low temperature, where *pp* pairing is also present, but they increase approaching the neutron critical temperature and then vanish. Quite interestingly, a jump is seen at $T = T_c^n$, when the cross section suddenly reaches the value of normal matter. A small jump also occurs,

for both proton fractions, at lower temperature, as a consequence of the disappearance of proton pairing. These jumps are related to the discontinuity which emerges, as in the heat capacity [14, 25], in the matter compressibility, that is in the chemical potential derivatives with respect to the density [14].

The conditions of panel (b) of fig. 3 are such that the q value considered corresponds to unstable fluctuations at zero temperature. A divergency occurs for the cross sections at the temperature associated with the crossing of the spinodal border. Also in this case a discontinuity is observed at the neutron critical temperature. Lastly, panels (c) and (d) of fig. 3 show the ratio R between the full calculations and the results obtained neglecting pairing correlations, to better evidence the amplitude of the pairing effects.

To conclude, our analysis highlights an important impact of superfluidity on neutrino transport properties, for thermodynamical conditions close to the spinodal border and characterized by quite large density fluctuations, which are of relevant interest for the evolution of newly formed neutron stars and supernovae explosion in the pre-bounce phase [24, 25]. We generally observe an enhancement of the neutrino differential cross section in paired matter and, consequently, of the neutrino trapping phenomenon. Moreover, a reduction in the energy flux carried out by neutrino emission is predicted and so new hints emerge about a significant impact of pairing on the cooling mechanism of low-density stellar matter at moderate temperature.

For sake of completeness, we mention that we recently showed that our finding is quite robust, since it does not depend very much on the in-medium suppression of the neutron BCS pairing gap so far adopted [27].

Despite the importance of this study, one should finally remark that more sophisticated analyses [11,28], going beyond our mean-field approximation, show that many-body correlations and clustering phenomena can actually modify the thermodynamical conditions of the low-density matter interacting with neutrinos. Moreover, it has been shown that the presence of large clusters may significantly influence the evaluation of pairing [29] in the inner crust of a neutron star. Work is therefore in progress to include these effects in our analysis.

REFERENCES

[1] Horowitz C. J. *et al.*, *Phys. Rev. C*, **86** (2012) 065806.
[2] Potekhin A. Y., Pons J. A. and Page D., *Space Sci. Rev.*, **191** (2015) 239.
[3] Janka H. T. *et al.*, *Phys. Rep.*, **442** (2007) 38.
[4] Baldo M. *et al.*, *Phys. Rev. C*, **89** (2014) 048801.
[5] Watanabe G. *et al.*, *Phys. Rev. C*, **68** (2003) 035806.
[6] Horowitz C. J., Pérez-García M. A. and Piekarewicz J., *Phys. Rev. C*, **69** (2004) 045804.
[7] Martínez-Pinedo G. *et al.*, *Phys. Rev. Lett.*, **109** (2012) 251104.
[8] Pais H., Newton W. G. and Stone J. R., *Phys. Rev. C*, **90** (2014) 065802.
[9] Chomaz Ph., Colonna M. and Randrup J., *Phys. Rep.*, **389** (2004) 263.
[10] Borderie B. and Rivet M. F., *Progr. Part. Nucl. Phys.*, **61** (2008) 551.
[11] Raduta Ad. R., Gulminelli F. and Aymard F., *Eur. Phys. J. A*, **50** (2014) 24.
[12] Margueron J., Navarro J. and Blottiau P., *Phys. Rev. C*, **70** (2004) 028801.
[13] Page D. *et al.*, *Astrophys. J.*, **707** (2009) 1131.
[14] Burrello S., Colonna M. and Matera F., *Phys. Rev. C*, **89** (2014) 057604.
[15] Baran V. *et al.*, *Phys. Rev. Lett.*, **86** (2001) 4492.
[16] Iwamoto N. and Pethick C. J., *Phys. Rev. D*, **25** (1982) 313.
[17] Burrows A. and Sawyer R. F., *Phys. Rev. C*, **58** (1998) 554.

[18] Landau L. D. and Lifshitz E. M., *Statistical Physics Part 1*, Vol. **5** (3rd edition) (Butterworth-Heinemann, Oxford) 1980.
[19] Chamel N., *Phys. Rev. C*, **82** (2010) 014313.
[20] Roca-Maza X. *et al.*, *Phys. Rev. C*, **87** (2013) 034301.
[21] Cao L. G., Lombardo U. and Schuck P., *Phys. Rev. C*, **74** (2006) 064301.
[22] Ducoin C., Chomaz Ph. and Gulminelli F., *Nucl. Phys. A*, **789** (2007) 403.
[23] Page D. and Reddy S., *Neutron Star Crust* (Nova Science Publishers, New York) 2012.
[24] Buyukcizmeci N. *et al.*, *Nucl. Phys. A*, **907** (2013) 13.
[25] Burrello S. *et al.*, *Phys. Rev. C*, **92** (2015) 055804.
[26] Colonna M. and Matera F., *Phys. Rev. C*, **71** (2005) 064605.
[27] Burrello S., Colonna M. and Matera F., *Phys. Rev. C*, **94** (2016) 012801.
[28] Typel S. *et al.*, *Eur. Phys. J. A*, **50** (2014) 17.
[29] Fortin M. *et al.*, *Phys. Rev. C*, **82** (2010) 065804.